32ND INTERNATIONAL COSMIC RAY CONFERENCE, BEIJING 2011

Hard X-ray/soft gamma-ray observations of the Galactic diffuse emission with INTEGRAL/SPI

LAURENT BOUCHET[1,2], ANDREW W. STRONG[3], TROY A. PORTER[4], IGOR V. MOSKALENKO[4], ELISABETH JOURDAIN[1,2], JEAN-PIERRE ROQUES[1,2]
[1] *Université de Toulouse, UPS-OMP, IRAP, Toulouse, France*
[2] *CNRS, IRAP, 9 Av. colonel Roche, BP 44346, F-31028 Toulouse cedex 4, France*
[3] *Max-Planck-Institut für extraterrestrische Physik, Postfach 1603, 85740 Garching, Germany*
[4] *Hansen Experimental Physics Laboratory, Stanford University, Stanford, CA 94305*
bouchet@cesr.fr
DOI: 10.7529/ICRC2011/V07/1320

Abstract: The spectrometer SPI, onboard the INTEGRAL observatory, gives us a unique opportunity to study the hard X-ray/soft gamma-ray diffuse emission. Based on a total observation time of $\sim 10^8$ s performed in more than 6 years of operation, we have measured a detailed ridge spectrum and constrained the spatial distribution of the emission from 20 keV to 2.5 MeV. The interstellar part of the ridge emission can be explained by inverse-Compton scattering from relativistic electrons on the cosmic microwave background and the Galactic infrared/optical radiation fields. The spectrum and its spatial distribution is compared with predictions from GALPROP modelling. We show also the potential of SPI data for determining the electron spectrum at low GeV energy where the solar modulation makes any direct measures of the electron spectrum difficult to interpret.

Keywords: Diffuse emission (Galactic and extragalactic)

1 Introduction

In our previous work, described in [1, 2], we have presented sky maps and spectra of the Galactic plane and demonstrated the presence of a hard power-law continuum emission, which was interpreted as inverse-Compton emission from cosmic-ray (CR) electrons and positrons upscattering the Galactic interstellar radiation field (ISRF).

In the present analysis, we take advantage of the greatly increased observational dataset and significant advances in the analysis techniques to derive the spatial morphology and the spectral shape of the Galactic diffuse emission.

2 Instument and observations

The European Space Agency's *INTEGRAL* observatory was launched from Baïkonour, Kazakhstan, on 2002 October 17.

The SPI spectrometer is equipped with an imaging system sensitive both to point sources and extended/diffuse emission with a field of view of 30° and 19 Ge detectors ([3]; [4]). Due to a non typical coded mask imaging system, SPI's imaging capability relies also on a specific observational strategy based on a dithering procedure [5].

Public data recorded between February 2003 and January 2009 with the INTEGRAL/SPI instrument are analyzed. It results in $\sim 1.1 \times 10^8$ s observation livetime which corresponds to $\sim$ 39000 exposures or pointings, excluding data contaminated by solar flares or the radiation belts.

3 Background and point sources variabilities modelling

The SPI background pattern (i.e. relative count rates of the detectors) is globally stable between Ge detector annealings (performed twice a year), but its intensity varies. However, this latter is quite stable on a $\sim$ 6-hour timescale.

Many sources exhibit variability on time scales ranging from one exposure ($\sim$2000 s) to years. For a given source, we divide its total observation period into smaller meaningful time intervals ("time bins") where it can be considered to have a constant flux within the error bars, using a segmentation code developped to achieve this task [6].

Due to the imaging system, it is imperative to process simultaneously a maximum of exposures (so-called mosaicking of images is not possible with SPI) to probe the lowest flux levels such as the diffuse emission. Finally, intensities in the source "time bins" and background intensity (each $\sim$6 hours) are the parameters fitted to the whole set of data (through the response matrix) to maximize the likelihood of the data as described in [7].

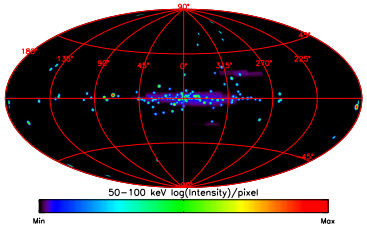

Figure 1: 50-100 keV intensity sky map including both sources and diffuse emission.

4 All-sky view of the Milky-Way

Point-sources contribution is extracted from the data, simultaneously with the diffuse and background components, and hence a census of sources is also derived. The resulting *INTEGRAL/SPI* all-sky survey allows us to detect $\sim$ 260 point sources. Figure 1 shows the 50-100 keV all sky map. Figure 3 compares the sum of sources emission to the diffuse spectrum, between 20 and 2500 keV.

5 Galactic emission spatial morphology

The diffuse emission over the whole sky has been imaged by extracting the flux contained in sky pixels. The pixels size habe been chosen to be relatively large ($\geq \delta l = 15^\circ \times \delta b = 2.6^\circ$) to avoid "cross-talk" effects with point sources.

We present our results in terms of longitude and latitude profiles (fig. 2). They have been built by integrating the flux measured for $|b| \leq 6.5^\circ$ in longitude or $|l| \leq 23^\circ$ in latitude (respectively $|b| \leq 8.2^\circ$ and $|l| \leq 60^\circ$ for the 600-1800 keV band).

A complementary analysis was performed in which the diffuse continuum spatial morphology is modelled using several template maps. Many combinations of templates were tested, the detailled procedure is decribed in [8].

Finally, above 600 keV, the Inverse-Compton (IC) map computed using GALPROP, (**Section 7**, hereafter IC) fits the data very well given the data statistics.

At energies below 600 keV, the situation is more complex. In addition to the diffuse continuum, we have the annihilation radiation spectrum whose bulge component is modeled by a combination of 3.2° and 11.8° Gaussians centred at $l = -0.6^\circ$ and $b = 0.0^\circ$ [7]. Good fits to the spatial morphology emission are obtained with a combination of IC and NIR/DIRBE 4.9μ (corrected from reddenning, hereafter 4.9μ) maps (plus a bulge component). Furthermore, the 4.9μ tracer is also consistent with the stellar origin for the Galactic ridge emission in the X-ray domain proposed by [11].

6 Spectral analysis of the diffuse emission

We have to fix a sky model to extract the spectral flux. Below 600 keV, the diffuse spectrum morphology is modelled as a linear combination of a 4.9μ and an IC map (Section 7) plus two Gaussians representing the bulge annihilation radiation component. At energies above 600 keV, the morphology is simply modelled by the IC map plus 3 spectral lines (^{26}Al (1.8 MeV), ^{60}Fe (1.17 and 1.33 MeV)).

In a first step, the summed components (sum of IC, 4.9μ and annihilation component) spectrum is directly fitted as a superposition of three expected physical spectral components:

- "Unresolved sources" emission, which dominates the emission below 50 keV, modelled by an exponential cutoff power-law spectrum.
- Annihilation radiation spectrum modelled by a Gaussian centered at 511 keV with 2.5 keV FWHM plus positronium continuum [10].
- Diffuse continuum mainly attributed to interstellar emission, modelled by a power law.

The power law component corresponding to the diffuse continuum, thought to be of interstellar origin, is then best fit by a power law of index $\sim$ 1.4-1.5 (fig. 3). This result is consistent with our previous work [1].

In a second step, each diffuse spatial component is directly decomposed into the three spectral components described above. From this analysis, the diffuse continuum power is seperated into two spatial components; the IC component having a power law index of 1.8 and the 4.9μ having a much harder power law index of $\sim$1. For the 4.9μ , a cutoff is introduced in order to steepen its contribution at higher energies (above 1 MeV).

The bulge annihilation radiation and the unresolved sources components are modelled as described above. An additional component, related to annihilation radiation emission disk spatial morphology is fitted by a combination of IC and 4.9μ maps. It cannot be properly separated from the power-law continuum, but it can be inferred from the model-fitting of the combined spectrum. The range of uncertainty of each extracted physical component is shown as a shaded area in fig. 3.

7 Modelling the diffuse emission

The GALPROP code [12] including a new model for the Galactic interstellar radiation field (ISRF) has been used to predict Galactic diffuse emission in the energy range from keV to TeV energies, thus covering more than 10 orders of magnitude in energy [2].

We use a model (GALPROP ID 54_z04LMS) based on the electron (plus positron) spectrum measured by *Fermi-LAT* [9], but not adjusted to *Fermi-LAT* gamma-ray data. It has a halo height of 4 kpc and includes CR reacceleration; for further details see [13].

Figure 4 compares the standard GALPROP model (54_z04LMS) with the spectrum measured by SPI; the

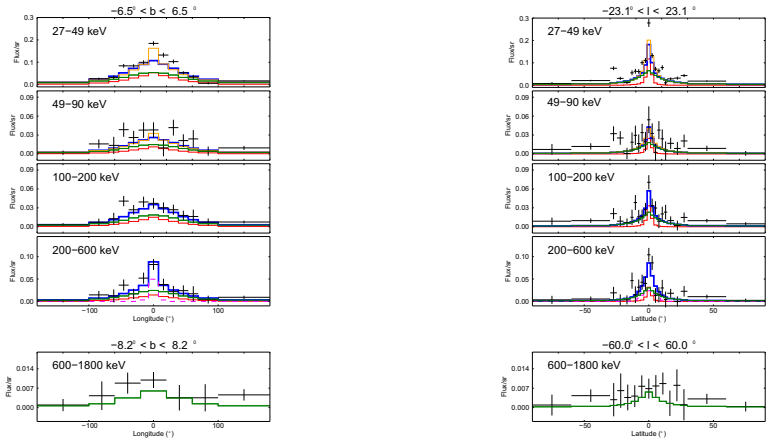

Figure 2: Longitude and laitude profiles of the Galactic Ridge emission in different energy bands, observed with *INTEGRAL/SPI*(crosses). The best fit template maps consiting of a combination of GALPROP Inverse-Compton (IC) distribution, 4.9μ and annihilation radiation contribution is shown in blue. 4.9μ (stellar emission) and IC contributions are shown respectively in red and green. The pink dash-dotted line is the annihilation radiation contribution in the 200-600 keV energy band. The orange thin line (best absolute model) is a model consisting of IC plus 4.9μ for energy below 49 keV and IC plus 60μ emission map between 49 keV and 200 keV. For this analysis, the channels containing ^{26}Al and ^{60}Fe lines are excluded from the data.

agreement with the spectral shape and in absolute flux is satisfactory given the uncertainties. Nevertheless, a better agreement with SPI is obtained with a higher electron spectrum (producing more IC emission) with the model 54_z04LMS_efactorS, where the spectrum is increased by a factor 2 over the standard model based on the electrons (plus positrons) measured by *Fermi-LAT*. This justifies the choice of model 54_z04LMS_efactorS as the standard inverse Compton model used throuhout this analysis. This can either be interpreted as the locally-measured spectrum being not typical of the global average at the solar position, but also as a cosmic-ray distribution more peaked towards the inner Galaxy than the (SNR and pulsar-based) distribution used in the standard GALPROP model.

Fig 4 shows other possibilities to increase the IC component, either by increasing the Galactic cosmic-ray halo height from 4 kpc to 10 kpc, or by increasing the ISRF by a factor of 10 in the Galactic bulge. A larger ISRF is suggested by a new analysis of COBE/DIRBE data T. Porter, private communication). The radial distribution of electrons is not well known or constrained, and a factor 2 increase of the electrons in the inner few kpc is still possible. The same effect could be obtained with secondary positrons if their progenitors (CR protons) increased by a similar factor. In anothe side, a larger halo is suggested by analysis of cosmic-ray data [14] and gamma rays [13]. Unfortunately, the morphology of these components would not be distinguishable by *INTEGRAL/SPI*.

Moreover, the photon energy range from 50 keV to 2 MeV is sensitive to IC from electrons below about 5 GeV, as it suppresses most of the photons in the SPI energy range. This demonstrates the potential of SPI data for determining the electron spectrum at low GeV energies where solar modulation makes interpretation of the directly-measured electron spectrum problematic. In fact observations of gamma-rays in this range could eventually be used to constrain models of solar modulation.

8 The 'Fermi bubbles'

Using *Fermi-LAT* data, a claim has been made for two large gamma-ray 'bubbles', extending 50° above and below the Galactic center, with a width of about 40° in longitude [15]. Above 50 keV, we found no emission corresponding to the bubbles (the 2σ upper limits for north or south bubble are 1.8, 1,3, 1.5 and 1.2 10^{-3}ph cm^{-2} s^{-1} respectively in the 50-100, 100-200, 20-600, 600-1800 keV bands).

9 Summary

The diffuse emission intensity in the central radian region ($|l| < 30°$, $|b| < 15°$) is estimated to be one tenth of the total emission (including sources) below 100 keV and one third in 100-300 keV band while the annihilation radiation spectrum dominates the sky emission between 250 and 511 keV. The diffuse emission spectrum has the following main features:

- The diffuse continuum spectrum (apart from positronium) is fitted by a power law of index 1.4 - 1.5 , with a flux at 100 keV of 1.1 $\times 10^{-4}$ ph cm^{-2} s^{-1} keV^{-1} . This power law, thought to be related to interstellar emission, can be decomposed into two spatial components: the IC component with a power law of index 1.8 and a flux at 100 keV of $\sim 10^{-4}$ ph cm^{-2} s^{-1} keV^{-1} , and an additional component which can be modelled with the 4.9μ template, and whose spectral shape is a power law with an very soft index of ~ 1 and a flux at 50 keV of $\sim 3 - 4 \times 10^{-5}$

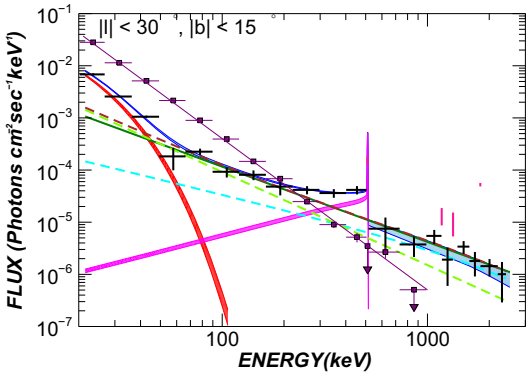

Figure 3: Spectra of the different emission components in the central radian of the Galaxy ($|l| < 30°$ and $|b| < 15°$). SPI measurements are black crosses. Violet squares: total emission of resolved sources. Violet line: power law fit to the resolved sources emission (power law index is 2.9 and flux at 100 keV is 4×10^{-4} ph cm^{-2} s^{-1} keV^{-1}). Blue: total diffuse emission – Magenta: annihilation radiation spectrum (line + positronium) – Red: Emission of low energy "unresolved" sources. The possible range of variation of these components are represented with the shaded area. Dark green line – is the deduced continuum emission thought to be dominated by interstellar particle interaction. The diffuse continuum best fit spectrum based both on spatial morphology and spectral decomposition is indicated by the dashed cyan (4.9μ spatial component) and green dashed lines (IC component). The sum of these two components is the brown dashed line which compared to the power law fit of index 1.44 based solely on spectral decomposition (dark green line).

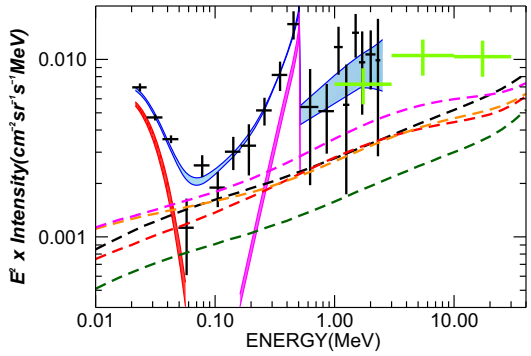

Figure 4: Same as figure 6 with different GALPROP configurations. The dashed dotted lines are IC models. Primary electron spectrum of fig 7 (dark green), primary electron spectrum increased by a factor 2 of fig 8 (black), increased halo height from 4 kpc to 10 kpc (red) and increased ISRF in the Galactic bulge (x 10) (orange) and both increased halo height from 4 kpc to 10 kpc and ISRF in the Galactic bulge (x 10) (magenta).

ph cm^{-2} s^{-1} keV^{-1} . This additional componentt steepens above $\sim$ 1 MeV (cutoff at $\sim$ 3.4 MeV) and is weak below 200 keV compared to the IC component.

- The diffuse continuum flux around 1 MeV is found compatible with the *COMPTEL/CGRO* measurement.
- The IC emission distribution predicted by the GALPROP code is in fair agreement with the data, but a model with an electron spectrum increased by a factor 2 over the standard model based on the electrons (plus positrons) measured by *Fermi-LAT* agrees better. An increased ISRF in the Galactic bulge or a large Galactic CR halo are other possibilities to obtain the increased flux.
- An additional component is required below 50 keV. This excess over the IC emission is well modeled with the NIR/DIRBE 4.9μ map. This low-energy component has an exponential spectrum with a cutoff at 8 keV and a flux at 50 keV of $\sim 2 \times 10^{-4}$ ph cm^{-2} s^{-1} keV^{-1} . It can thus be directly interpreted in term of stellar origin as proposed by [11].

In addition, we found that our global diffuse spectrum is consistent through the measured characteristics of nuclear lines (^{26}Al, ^{60}Fe) and annihilation radiation spectrum.

There is no detection in the SPI energy range of the 'Fermi bubbles'.

In the future, SPI will continue to provide new data for, at least, the next 3 years. Meanwhile, the Fermi Gamma Ray Space Telescope is providing new information on the Galactic spectrum at higher energies, and *INTEGRAL* gives complementary measurements related to the same physical processes. Taken together the data from the two missions, and including already existing data, will constrain the cosmic-ray electron spectrum at all energies and help to give an unambiguous decomposition of the diffuse γ-ray sky.

References

[1] Bouchet, L. et al., *ApJ* , 2008, 679, 1315
[2] Porter, T. et al., *ApJ* , 2008, 682, 400
[3] Roques, J. P. et al., *A & A* , 2003, 411, L91
[4] Vedrenne, G. et al., *A & A* , 2003, 411, L63
[5] Jensen, P. L. et al., *A & A* , 2003, 411, L7
[6] Bouchet, L., et al., 2011, in preparation
[7] Bouchet, L., Roques, J. P., & Jourdain, E., *ApJ* , 2010, 720, 1772
[8] Bouchet, L., et al., *ApJ* , 2011, submitted
[9] Abdo, A. A., et al., Phys. Rev. Lett., 2010, 104, 10, id. 10110
[10] Ore, A. & Powell, J. , Phys. Rev., 1949, 75, 1696
[11] Krivonos, R., et al., *A & A* , 2007, 463, 957
[12] Strong, A. W., Moskalenko, I. V., & Ptuskin, V. S., Ann. Rev. Nucl. Part. Sci., 2007, 57, 285
[13] Strong, A.W., 2010, Proceedings of the ICATPP Conference on Cosmic Rays for Particle and Astroparticle Physics, to be published by World Scientific (Singapore), arXiv:1101.1381.
[14] Trotta R. L., et al., *ApJ* , 2010, 729, 106
[15] Su, M., Slatyer, T. R., &Finkbeiner, D. P., *ApJ* , 2010, 724, 1044

OG.2.2: Galactic sources (Binaries, micro quasars, pulsars, SN remnants, molecular clouds, etc.)